

# The mechanism of CCN1-enhanced retinal neovascularization in oxygen-induced retinopathy through PI3K/Akt–VEGF signaling pathway

Yu Di<sup>1</sup>Yiou Zhang<sup>2</sup>Hongwei Yang<sup>1</sup>Aiyuan Wang<sup>1</sup>Xiaolong Chen<sup>1</sup>

<sup>1</sup>Department of Ophthalmology, Shengjing Affiliated Hospital of China Medical University, Shenyang, People's Republic of China; <sup>2</sup>Graduate School, China Medical University, Shenyang, People's Republic of China

**Background:** CCN1 (also called Cyr 61) is an extracellular matrix signaling molecule that has been implicated in neovascularization through its interactions with several endothelial integrin receptors. The roles of vascular endothelial growth factor (VEGF) in angiogenesis are well described. The aim of this study was to investigate the signal transduction mechanism of CCN1–PI3K/Akt–VEGF in retinopathy of prematurity (ROP), and the effects of CCN1 knockdown on ROP.

**Methods:** The oxygen-induced retinopathy (OIR) model was established in C57BL/6J mice exposed to a high concentration of oxygen. Retinas were obtained from the normoxia, OIR, OIR control (treated with scramble siRNA) and OIR treated (with CCN1 siRNA) groups. Retinal neovascularization (RNV) was qualitatively analyzed with ADPase staining and quantitatively analyzed by counting neovascular endothelial cell nuclei at postnatal day 17 when RNV reached a peak. mRNA level and protein expression of CCN1, p-Akt, and VEGF were measured by real-time PCR and Western blotting, and located with immunohistochemistry.

**Results:** CCN1 depletion resulted in less neovascularization clock hour scores in the number of preretinal neovascular cells compared with the OIR treated group ( $1.28 \pm 0.83$  versus  $4.80 \pm 0.82$ ; and  $7.12 \pm 2.50$  versus  $23.25 \pm 2.35$ , respectively, both  $P < 0.05$ ). Furthermore, CCN1, p-Akt and VEGF mRNA, and protein were significantly expressed in the retina of the OIR and OIR control groups. Intravitreal injection of CCN1 siRNA significantly reduced PI3K/Akt–VEGF pathway expression of the OIR mouse model (all  $P < 0.05$ ). CCN1 siRNA significantly enhanced the avascular area and avascular diameter of OIR model ( $P < 0.05$ ). CCN1 siRNA decreased the levels of IL-1 $\beta$ , IL-6, and TNF- $\alpha$  significantly compared to the OIR group ( $P < 0.05$ ).

**Conclusion:** These results suggest that CCN1 plays an important role in RNV via the PI3K/Akt–VEGF signaling pathway. CCN1 may be a potential target for the prevention and treatment of ROP.

**Keywords:** cysteine-rich 61, retinal neovascularization, retinopathy of prematurity, vascular endothelial growth factor

## Introduction

Retinal neovascularization (RNV) occurs in many proliferative ischemic retinopathies such as retinopathy of prematurity (ROP), proliferative diabetic retinopathy, and retinal vein occlusion.<sup>1</sup> At present, ROP is a leading cause of blindness among children in both developed and developing countries.<sup>2,3</sup> Therefore, the prevention and treatment of ROP have become an important task of ophthalmic physicians. Current therapies aim at eliminating/reducing the actual causes of RNV while simultaneously normalizing the retinal vasculature.<sup>4</sup>

It is now apparent that VEGF is a prominent factor in ROP that stimulates endothelial cell proliferation and tube formation and mediates ischemia-induced RNV.<sup>5–8</sup>

Correspondence: Xiaolong Chen  
Department of Ophthalmology,  
Shengjing Affiliated Hospital of China  
Medical University, Heping district,  
Sanhao Road 36, Shenyang 110004,  
People's Republic of China  
Tel +86 189 4025 1892  
Email chenxiaolongsy@yeah.net

Therefore, understanding the transcriptional regulation of VEGF may contribute to exploring the role of transcriptional regulators in RNV.

CCN1, or Cyr 61, is a secreted heparin-binding protein of 40 kDa that displays pro-angiogenic activities, including endothelial cell adhesion, migration, proliferation, and tubule formation.<sup>9–11</sup> Recent studies have demonstrated that CCN1 induces MCP-1 through the activation of PI3K/Akt and NF- $\kappa$ B signaling in chorioretinal vascular endothelial cells.<sup>12</sup> Additionally, a previous study showed that CCN1 via PI3K/Akt signaling pathway could enhance VEGF expression and promote tumor neovascularization.<sup>13</sup> However, the correlation of CCN1 and VEGF expression in ROP has not been elucidated and the actual mechanism of CCN1 in RNV of ROP remains unclear.

Therefore, we hypothesize that the CCN1–PI3K/Akt–VEGF signaling pathway might promote RNV of ROP. To test this hypothesis, we measured the expression of CCN1–PI3K/Akt–VEGF pathway in RNV. In addition, we investigated whether the block of CCN1 inhibited RNV of ROP.

## Materials and methods

### Animals

All experiments were performed in accordance with guidelines set by the Animal Experiment Committee of the Shengjing Hospital of China Medical University, and the study was approved by Shengjing Hospital of China Medical University's Ethics Committee. Throughout the study, C57BL/6J newborn mice (Animal Laboratory, China Medical University, Shenyang, People's Republic of China; female or male; n=280) were given access to food and water ad libitum and housed with lactating female mice.

### Oxygen-induced retinopathy

Oxygen-induced retinopathy (OIR) was induced in C57BL/6J mice as described by Smith et al.<sup>14</sup> Postnatal day 7 (P7) mice and their mothers were placed in a chamber and exposed to an

oxygen concentration of 75% $\pm$ 2% as monitored by an oxygen analyzer for 5 days (P12). The mice were exposed to 12-hour cyclical broad spectrum light. The room temperature was maintained at 23°C $\pm$ 2°C. On P12, the mice were removed to room air until P17, when the retinas were assessed for maximum neovascular response, as previously observed.<sup>14</sup>

The mice were randomly divided into four groups of 70: normoxia, OIR, OIR control (transiently transfected with the scramble siRNA), and OIR treated (transiently transfected with the CCN1 siRNA). The OIR control or treated groups received an intravitreal injection of 1  $\mu$ L scramble siRNA plasmid or CCN1 siRNA plasmid at P11 using a 33-gauge needle attached to a Hamilton syringe, and were returned to room air at P12. Mice in all four groups were deeply anesthetized with ketamine, and were sacrificed at P17 to collect retinas for morphological and pathological studies, as well as for mRNA and protein analyses.

### Preparation of CCN1 siRNA

CCN1 and scrambled siRNA were purchased from GenePharma Co. Ltd. (Shanghai, People's Republic of China). The sequence of siRNAs targeting the mouse CCN1 gene is shown in Table 1. The resultant siRNA was purified, quantified, and suspended in water at a concentration of 500 ng/ $\mu$ L; 0.5  $\mu$ L siRNA for CCN1 was combined with 0.5  $\mu$ L Lipofectamine 2000 (with the final concentration of Lipofectamine 2000 at 50 nM, and our preliminary results showed that this concentration is not toxic for in vitro and vivo both) (Thermo Fisher Scientific, Waltham, MA, USA) for 20 minutes before injection according to the manufacturer's instructions. The CCN1-homo-1072 construct yielded the best results, and was used in the following experiments.

### Angiography using ADPase

Retinal vascular patterns were assessed as previously described.<sup>15</sup> Eyes were enucleated and fixed in 4% paraformaldehyde for 3 hours. Retinas were dissected,

**Table 1** Sequences of the siRNAs targeting mouse CCN1 gene

Target gene	Position in gene	Sequences (5'-3')
CCN1	553	Sense: 5'-GGG AAAGUUUCCAGCCCA ACUTT-3'
		Antisense: 5'-AGUUGGGCUGGA AACUUUCCCTT-3'
	789	Sense: 5'-GAGGUGGAGUUG ACGAGA AACTT-3'
		Antisense: 5'-GUUUCUCGUCAACUCCACCUCTT-3'
	1,072	Sense: 5'-GCAAGAAAUGCAGCAAGACCATT-3'
		Antisense: 5'-UGGUCUUGCUGCAUUUCUUGCTT-3'
	1,268	Sense: 5'-GAUGAUCCAGUCCUGCAAUGTT-3'
		Antisense: 5'-CAUUUGCAGGACUGGAUCAUCTT-3'
Scrambled siRNA		Sense: 5'-UUCUCCGAACGUGUCACGUTT-3'
		Antisense: 5'-ACGUGACAGUUCGCGAGAATT-3'

flat-mounted through four incisions dividing them into four quadrants, and processed for magnesium-activated ADPase staining. Images were taken at 40× magnification on an Olympus B201 optical microscope (Olympus Corporation, Tokyo, Japan). Each retina was divided into 12 equal segments under the microscope, counting neovascularization clock hour scores, regardless of the number in each quadrant neovascularization.<sup>16</sup> Three independent reviewers were blinded to grouping when counting clock hour scores in order to assess the severity of neovascularization.

## Quantification of pre-RNV

To quantify preretinal neovascular cells, retinal structures were analyzed on 6 µm hematoxylin and eosin-stained section as described previously.<sup>17</sup> At P17, the eyes were enucleated and fixed in 4% paraformaldehyde for 24 hours, and embedded in paraffin. Serial sections (6 µm) of whole eyes were cut sagittally through the cornea and parallel to the optic nerve and stained with hematoxylin and eosin. Ten nonserial sections were analyzed per eye. The preretinal neovascular cell nuclei, identified under light microscopy, was considered to be associated with new vessels if they were found on the vitreal side of the internal limiting membrane (ILM).<sup>17</sup> Three independent reviewers were blinded to grouping when counting the cells.

## Immunohistochemistry analysis

Formalin-fixed, paraffin-embedded 6 µm eye tissue sections were placed on slides, deparaffinized in xylene, and rehydrated in graded ethanol baths in phosphate-buffered saline. Immunostaining was performed by the streptavidin-peroxidase method (Ultrasensitive; MaiXin, Fuzhou, People's Republic of China). Hydrogen peroxide (3%) was applied to block endogenous peroxidase activity, and normal goat serum was used to reduce nonspecific binding.

Sections were incubated with commercially available primary antibodies: rabbit anti-CCN1 polyclonal antibody (1:500, Abcam, Cambridge, UK); rabbit anti-p-AKT1/2/3 (Ser473) polyclonal antibody (1:500, Santa Cruz Biotechnology Inc., Dallas, TX, USA); or rabbit anti-VEGF polyclonal antibody (1:500, Santa Cruz Biotechnology Inc.) overnight at 4°C. The sections were incubated with biotinylated secondary antibody (1:1,000, Santa Cruz Biotechnology Inc.) and reacted with the avidin-biotinylated peroxidase complex. The primary antibody was replaced with phosphate-buffered saline for negative controls. The peroxidase reaction was developed with 3, 3'-diaminobenzidine (Maixin Biotechnology, Foshan, China), and sections

were counterstained with hematoxylin, dehydrated with alcohol, and mounted using a standard procedure. Images were digitally captured using an Olympus B201 optical microscope.

## Western blot analysis

For protein analysis from retinas, mouse eyes were enucleated and retinas were carefully dissected and homogenized in lysis buffer containing 50 mM Tris-HCl (pH 8.0), 150 mM NaCl, 0.5% Nonidet P40, 0.5% sodium deoxycholate, and phenylmethylsulfonyl fluoride (all from Sigma-Aldrich Co., St Louis, MO, USA). Protein samples (30 µg) were run on 10% sodium dodecyl sulfate polyacrylamide gel electrophoresis and transferred to polyvinylidene fluoride membranes (Merck Millipore, Billerica, MA, USA). After blocking with 5% bovine serum albumin in Tris-buffered saline-Tween 20 (TBST; 20 mM Tris-HCl, 500 mM NaCl, 0.05% Tween-20), membranes were incubated with specific primary antibodies, including rabbit anti-CCN1 polyclonal antibody (1:2,000, Abcam); rabbit anti-pAkt1/2/3 polyclonal antibody (1:2,000, Santa Cruz Biotechnology Inc.); mouse anti-IL-1β monoclonal antibody (1:3,000, Santa Cruz Biotechnology Inc.), rabbit anti-IL-6 polyclonal antibody (1:1,000, Abcam), mouse anti-TNF-α monoclonal antibody (1:3,000, Santa Cruz Biotechnology Inc.) or rabbit anti-VEGF polyclonal antibody (1:2,000, Santa Cruz Biotechnology Inc.) overnight at 4°C, followed by incubation with horse-radish-peroxidase-conjugated secondary antibody (1:2,000, Zhongshan Jinqiao Biotechnology Co. Ltd., Beijing, People's Republic of China) for 1 hour. Signals were detected with enhanced chemiluminescence (Pierce Biotechnology, Rockford, IL, USA) in the GIS-2020 image-processing system (Technew Tech. Co. Ltd., Shanghai, People's Republic of China). The ratio between the optical density of the protein of interest and β-actin of the same sample was calculated as the relative content of the protein detected.

## Quantitative real-time RT-PCR

Total RNA was isolated using RNAiso Plus (Takara Bio, Otsu, Japan). Quantitative real-time RT-PCR (qRT-PCR) was performed using the reverse transcriptase kit from Takara Bio (PrimeScript RT Reagent Kit-Perfect Real Time) (Takara Bio, Otsu, Japan). Primers were designed using Primer Express software, version 2.0 (Thermo Fisher Scientific). β-actin was used as a normalizing control. The primers used in the retinas are shown in Table 2. Quantitative real-time PCR was performed using the SYBR Green PCR Master Mix (Premix Ex Taq Perfect Real Time; Takara Bio) in a total volume of 20 µL on a 7300 Real-Time PCR System

**Table 2** Primer sequences for qRT-PCR

Gene	Primer sequences (5'-3')	Product length (bp)	Tm (°C)
β-actin	Forward CCT CCT CCT GAG CGC AAG TA	117	55
	Reverse GAT GGA GGG GCC GGA CT		
VEGF	Forward CCC GAC AGG GAA GAC AAT	131	55
	Reverse TCT GGA AGT GAG CCA ACG		
Akt	Forward AGC AAA CAG GCT CAC AGG TT	245	55
	Reverse TAA GTC CTC CCC ATG TCC CT		
CCN1	Forward AGA CCC TGT GAA TAT AAC TCC A	300	55
	Reverse AAT TGC GAT TAA CTC ATT GTT T		

**Abbreviations:** qRT-PCR: quantitative real-time PCR; VEGF, vascular endothelial growth factor; Tm, temperature; bp, base pair.

(Thermo Fisher Scientific): 95°C for 30 seconds, 50 cycles of 95°C for 5 seconds, and 60°C for 31 seconds. Relative quantification of the gene expression was performed using the  $2^{-\Delta\Delta Ct}$  method.<sup>18</sup>

## Statistical analysis

SPSS version 13.0 software was applied to complete data processing. All data were represented as mean  $\pm$  standard deviation (SD). Statistical significance was evaluated by one-way analysis of variance with the least significant difference test for post hoc analysis.  $P < 0.05$  was considered statistically significant.

## Results

### Qualitative assessment of RNV

To determine whether CCN1 siRNA suppresses oxygen-induced ischemic RNV, we examined the retinal vasculature of the normoxia, OIR, OIR control, and OIR treated groups using ADPase in retinal flat mounts at P17 (Figure 1). The retinas of the normoxia group had both superficial and deep vascular layers that extended from the optic nerve to the periphery. The vessels formed a fine radial branching pattern in the superficial retinal layer and a polygonal reticular pattern in the deep retinal layer. The retinal vessels of the OIR and

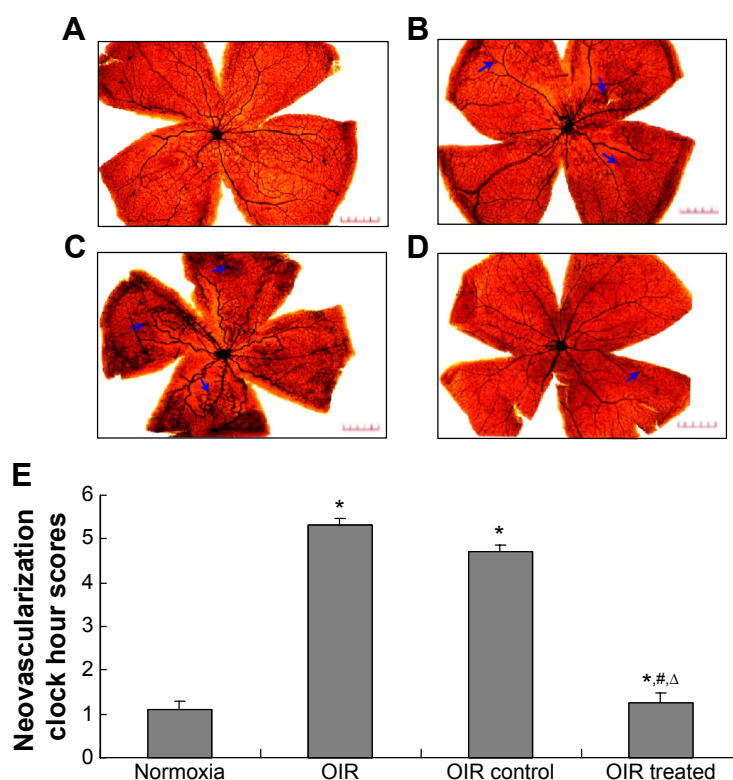


**Figure 1** Inhibitory effect of CCN1 siRNA on RNV in the OIR model.

**Notes:** The images are representative retinal angiographs from the eyes of the normoxia (A), OIR (B), OIR control (C), and OIR treated group (D). The statistical analysis result was illustrated in (E). The blue arrows indicate neovascularization (magnification: 40 $\times$ , bar: 50  $\mu$ m). Three independent reviewers were blinded to grouping when counting clock hour scores in order to assess severity of RNV. Data are shown as mean  $\pm$  SD (n=15). \* $P < 0.05$  versus the normoxia group, # $P < 0.05$  versus the OIR group, and  $\Delta P < 0.05$  versus the OIR control group.

**Abbreviations:** RNV, retinal neovascularization; OIR, oxygen-induced retinopathy; SD, standard deviation.



OIR control groups had an obvious dilation pattern extending from the optic nerve and larger regions of non-perfusion. Neovascular tufts extended from the surface of the retina at the junction between the perfused and non-perfused retina in the OIR group ( $5.20 \pm 0.75$ ) and OIR control group ( $4.80 \pm 0.82$ ), which was still higher than in the normoxia group ( $1.10 \pm 0.55$ ) (all  $P < 0.05$ ). In contrast, retinas of the OIR treated group ( $1.28 \pm 0.83$ ) developed less severe neovascular tufts and regions of non-perfusion compared with the OIR and OIR control groups (all  $P < 0.05$ ), which showed a strong inhibitory effect on RNV in the gene therapy group.

## Quantitative assessment of RNV

To confirm the inhibitory effect of CCN1 siRNA, examination of 6  $\mu\text{m}$  paraffin-processed cross-sections of mouse eyes was performed. The preretinal neovascular cells growing into

the vitreous humor were counted from each eye following an established method.<sup>17</sup> As shown in Figure 2, there was an average of  $0.98 \pm 0.20$  nuclei per cross-section in the normoxia group compared to  $25.55 \pm 2.84$  and  $23.25 \pm 2.35$  in the OIR and OIR control group, respectively (both  $P < 0.05$ ). Moreover, the average number of preretinal neovascular cells in the OIR treated group ( $7.12 \pm 2.50$ ) decreased significantly compared with the OIR and OIR control group (both  $P < 0.05$ ), confirming the anti-neovascularization effect of CCN1 siRNA on RNV in the gene therapy group.

Furthermore, in order to compare with the conventional VEGF therapy, we also examined the avascular area ( $\text{mm}^2$ ) and avascular diameter (mm) of every group. The results indicated that the avascular area and avascular diameter in the OIR and OIR control group were significantly decreased compared to the normoxia group (Figure S1,  $P < 0.05$ ). Also,

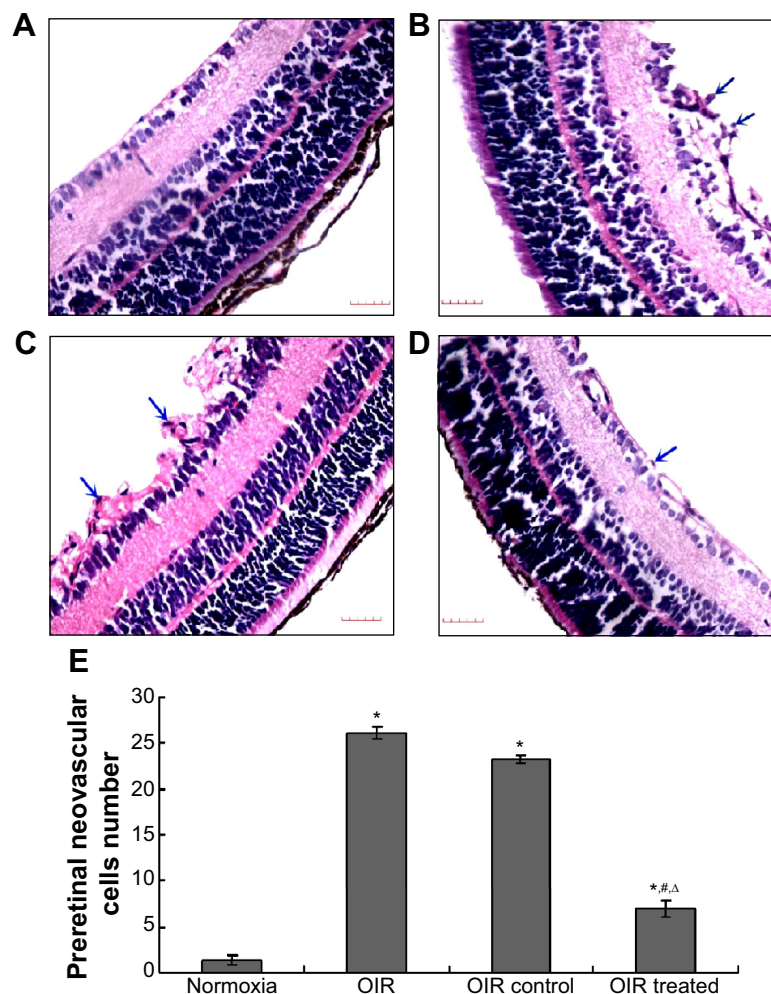


**Figure 2** Effect of CCN1 siRNA on pre-RNV in mice with OIR.

**Notes:** Preretinal neovascular cells were counted on ten non-continuous sections per eye, 15 eyes per group, and averaged. The images were representative retinal sections from the normoxia (A), OIR (B), OIR control (C), and OIR treated group (D). The statistical analysis result was illustrated in (E). The blue arrows indicate preretinal neovascular cells (magnification: 400 $\times$ , bar: 50  $\mu\text{m}$ ). Three independent reviewers were blinded to grouping when counting the cells. Data are shown as mean  $\pm$  SD (n=150). \* $P < 0.05$  versus normoxia group, # $P < 0.05$  versus OIR group, and  $\Delta P < 0.05$  versus OIR control group.

**Abbreviations:** RNV, retinal neovascularization; OIR, oxygen-induced retinopathy; SD, standard deviation.

the avascular area and avascular diameter in OIR treated group was significantly enhanced compared to the OIR and OIR control group (Figure S1,  $P < 0.05$ ), and even achieved the level of the normoxia group.

### CCN1–PI3K/Akt–VEGF signaling pathway of the OIR mouse model revealed by immunohistochemistry

Immunohistochemistry was performed to investigate the localization and expression levels of CCN1, p-Akt, and VEGF in the normoxia, OIR, OIR control, and OIR treated groups (Figure 3). Immunohistochemistry staining of retinal sections revealed CCN1, p-Akt, and VEGF expression was weakly detected only in the ganglion cell layer (GCL) and inner plexiform layer (IPL) of the normoxia group, whereas in the OIR and OIR control groups, they were strongly detected in the GCL, IPL, inner nuclear layer, and outer plexiform layer, with neovascularization breaking through the ILM. However, CCN1, p-Akt, and VEGF showed low-level expression in the

GCL and IPL and RNV breaking through the ILM of the OIR treated group compared with the OIR qRT-PCR: quantitative real-time PCR, and OIR control groups. The results demonstrated that hypoxia-induced CCN1 expression was mediated through the PI3K/Akt–VEGF pathway.

### CCN1 siRNA inhibited RNV through inhibiting PI3K/Akt–VEGF signaling in OIR mice, by real-time RT-PCR and Western blotting

Real-time RT-PCR demonstrated that CCN1, Akt, and VEGF mRNA levels in the OIR treated group were reduced by 64.58%, 50.87%, and 65.90%, respectively, when compared with the OIR control group (all  $P < 0.05$ , Figure 4). In addition, the expression of these mRNAs in the OIR and OIR control groups was upregulated significantly compared to the normoxia group (all  $P < 0.05$ , Figure 4), whereas there was no significant difference between the OIR and OIR control groups (all  $P > 0.05$ , Figure 4).

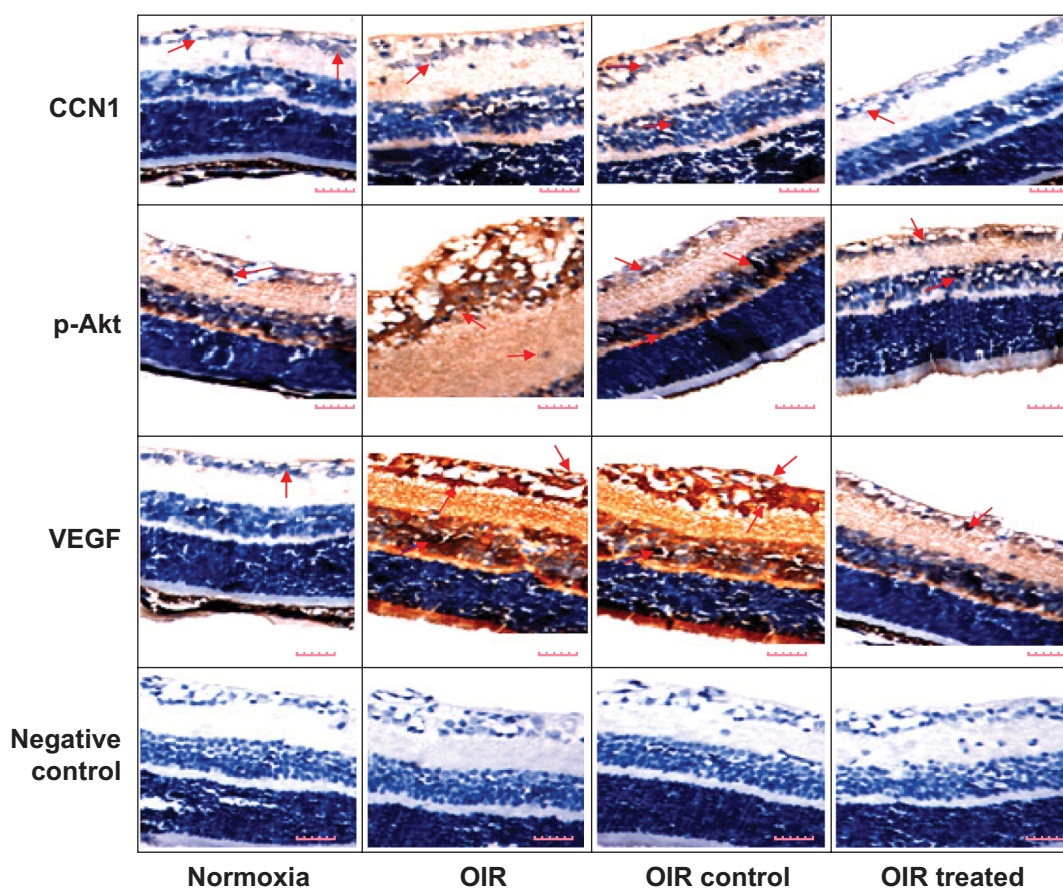


**Figure 3** Hypoxia-induced CCN1 expression was mediated through the PI3K/Akt–VEGF pathway in the OIR mouse model.

**Notes:** Protein expression of CCN1, p-Akt, and VEGF was determined by immunohistochemistry (magnification: 400 $\times$ , bar: 50  $\mu$ m). Red arrows: CCN1, p-Akt or VEGF positive cells.

**Abbreviations:** OIR, oxygen-induced retinopathy; VEGF, vascular endothelial growth factor.

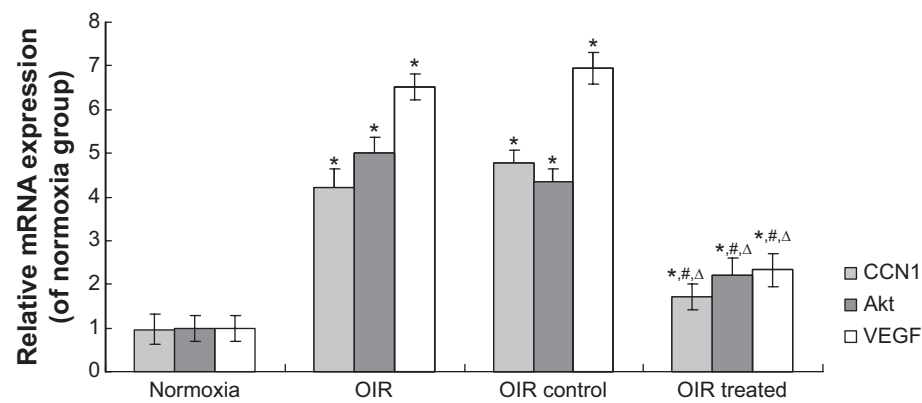


**Figure 4** CCN1 siRNA inhibited RNV through inhibition of the mRNA expression in PI3K/Akt-VEGF signaling pathway in the OIR mouse model.

**Notes:** mRNA expression of CCN1, Akt, and VEGF was determined by real-time RT-PCR. Data are shown as mean  $\pm$  SD (n=10). \* $P$ <0.05 versus normoxia group, # $P$ <0.05 versus OIR group,  $\Delta$  $P$ <0.05 versus OIR control group.

**Abbreviations:** RNV, retinal neovascularization; OIR, oxygen-induced retinopathy; SD, standard deviation; VEGF, vascular endothelial growth factor; qRT-PCR: quantitative real-time PCR.

Western blotting revealed similar results in retina samples. CCN1, p-Akt, and VEGF protein levels in the OIR treated group were reduced by 51.55%, 32.36%, and 45.70%, respectively, when compared with the OIR control group (all  $P$ <0.05, Figure 5). In addition, protein expression in the OIR and OIR control groups was upregulated significantly

compared to the normoxia group (all  $P$ <0.05, Figure 5), whereas there was no significant difference between the OIR and OIR control groups (all  $P$ >0.05, Figure 5).

Taken together, our results suggest that CCN1 siRNA inhibits RNV through inhibiting the PI3K/Akt-VEGF signaling pathway.

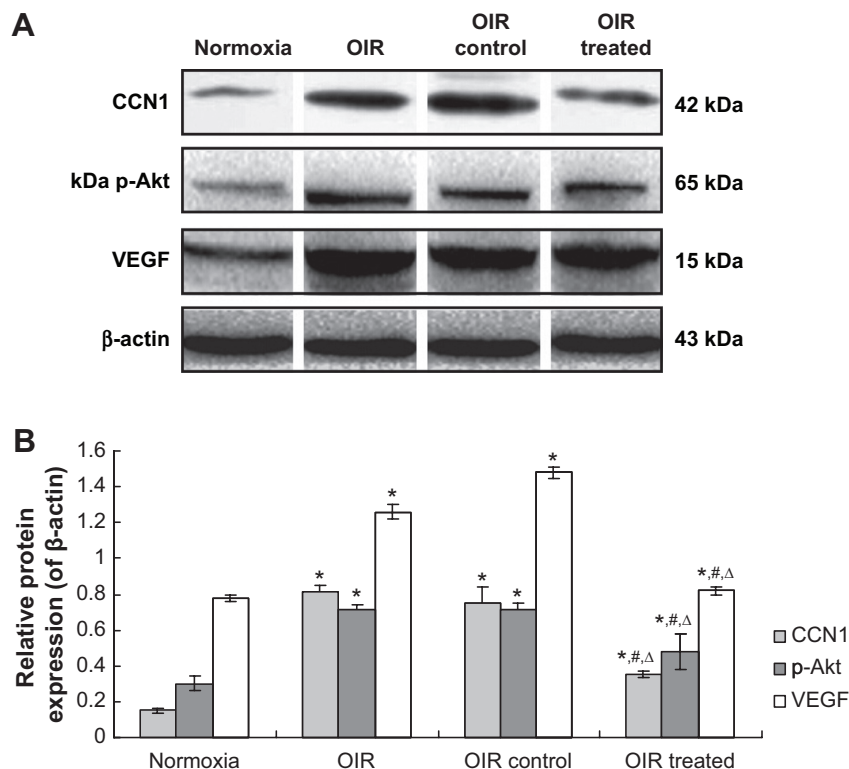


**Figure 5** CCN1 siRNA inhibited RNV through inhibition of the protein expression in PI3K/Akt-VEGF signaling pathway in the OIR mouse model. (A). Western blot assay for protein expression (B). Statistical analysis.

**Notes:** Protein expressions of CCN1, p-Akt, and VEGF were determined by Western blotting. Protein expression were normalized to  $\beta$ -actin. Data are shown as mean  $\pm$  SD (n=10). \* $P$ <0.05 versus normoxia group, # $P$ <0.05 versus OIR group,  $\Delta$  $P$ <0.05 versus OIR control group.

**Abbreviations:** RNV, retinal neovascularization; OIR, oxygen-induced retinopathy; SD, standard deviation; VEGF, vascular endothelial growth factor.

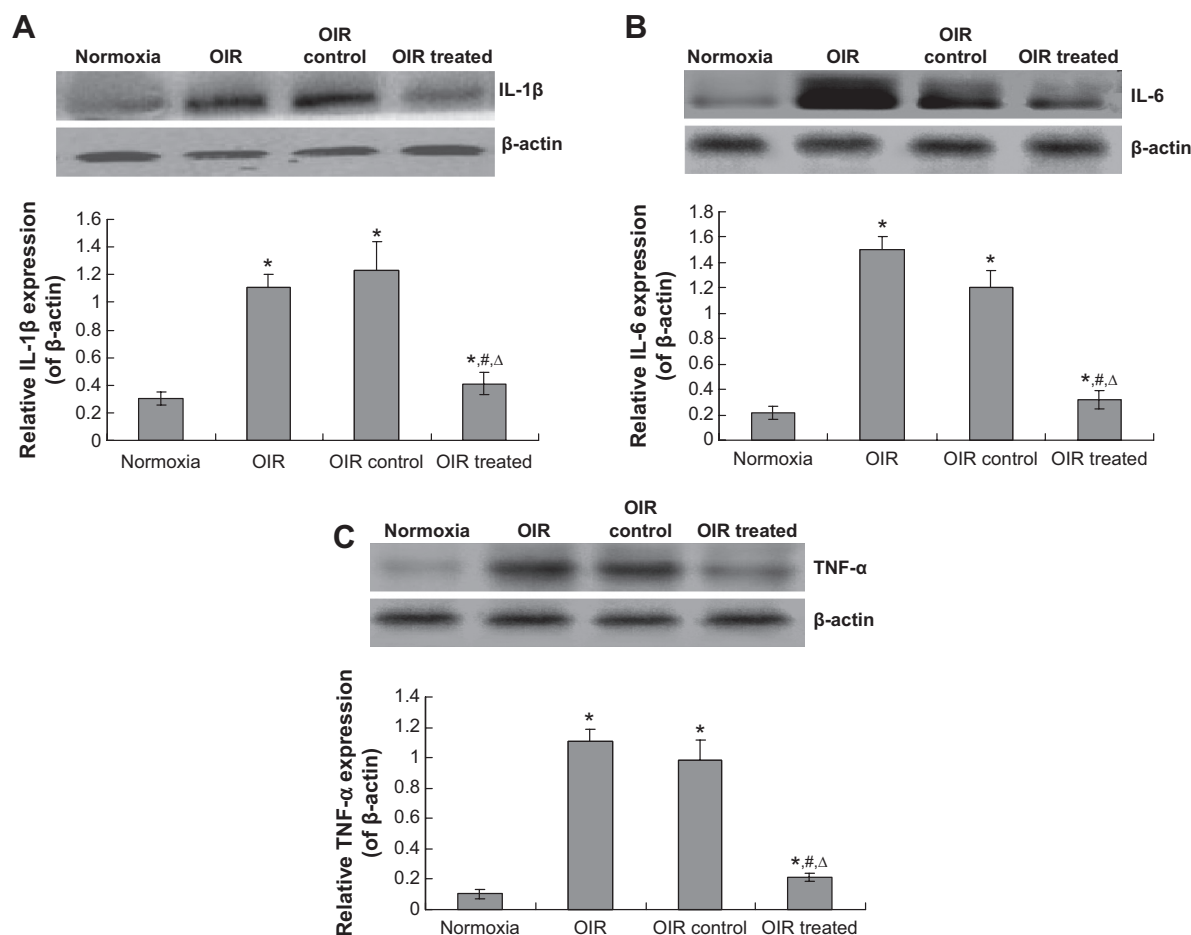


**Figure 6** CCN1 siRNA decreases the inflammatory cytokines expression.

**Notes:** Protein expression of IL-1β (A), IL-6 (B), and TNF-α (C) was determined by Western blotting, and analyzed with SPSS software. Protein expression was normalized to β-actin. Data are shown as mean ± SD (n=10). \**P*<0.05 versus normoxia group, #*P*<0.05 versus OIR group, Δ*P*<0.05 versus OIR control group.

**Abbreviations:** OIR, oxygen-induced retinopathy; SD, standard deviation; TNF-α, tumor necrosis factor α.

## CCN1 siRNA decreased the inflammatory response

In order to investigate the effects of CCN on the inflammatory response, the IL-1β, IL-6, and TNF-α were examined. The result indicated that there were serious inflammatory cytokines in the OIR and OIR control group compared to the normoxia group (Figure 6, *P*<0.05). However, the CCN1 siRNA decreased the levels of IL-1β, IL-6, and TNF-α significantly compared to the OIR group (Figure 6, *P*<0.05). These results suggest that the CCN therapy could also decrease the inflammatory response.

## Discussion

RNV is stimulated by one or more angiogenic factors released by the retina under ischemic or hypoxic conditions.<sup>19,20</sup> VEGF has been demonstrated to be a major pathogenic factor and therapeutic target in retinal angiogenic diseases.<sup>21</sup> Recent studies have demonstrated that intravitreal injection

of anti-VEGF antibody (bevacizumab or ranibizumab) is effective.<sup>22,23</sup> In addition, a previous study showed that intravitreal bevacizumab as an anti-VEGF monotherapy had a significant benefit for zone I ROP as compared with conventional laser therapy.<sup>24</sup> It is possible that several other factors participate in the angiogenic process involved in ROP. The candidate factors include bFGF,<sup>25</sup> HIF-1α,<sup>26</sup> and CCN family proteins.<sup>4,27</sup>

CCN1, the first cloned member of the CCN family, can also regulate the expression of genes involved in angiogenesis and matrix remodeling, including VEGF, MMP, and TIMPs.<sup>28,29</sup> Previous studies have shown potent pro-angiogenic properties of CCN1 in a rat cornea and diabetic retinopathy model.<sup>30,31</sup> Recent studies have also shown that the vitreous levels of CCN1 are upregulated in patients with proliferative diabetic retinopathy.<sup>32</sup> Therefore, CCN1 may induce RNV in OIR both directly and indirectly. However, few studies have elucidated the relationship between



CCN1 and VEGF on RNV in the OIR model. Our study found that expression of CCN1 and VEGF was increased to the same level in ischemic retina of OIR, thus verifying that CCN1 and VEGF can participate in the pathological process of ROP.

In this study, we also examined the avascular area and avascular diameter in every group. The results indicated that the CCN1 siRNA could increase the avascular area and avascular diameter in the ischemic retina of OIR. However, this effect could not affect the normal avascular area and avascular diameter compared to the conventional anti-VEGF. Therefore, the method in our study may replace the conventional anti-VEGF drugs in clinical for the ROP.

RNA interference is a powerful tool for post-transcriptional gene silencing, and is a new method to study gene function.<sup>33</sup> A previous study has shown that transfer of the siRNA gene to the retina was accomplished at 1 day after intravitreal injection.<sup>19,34</sup> For this reason, we delivered siRNA to the retina 1 day before the onset of hypoxia. We observed no endophthalmitis, systemic toxic reactions or death in the OIR control and OIR treated groups, thus, intravitreal injection of siRNA is safe and effective. In the present study, CCN1 siRNA intravitreal injection efficiently inhibited retinal angiogenesis by reducing VEGF mRNA and protein expression. These results confirm that CCN1 depletion can exert an anti-angiogenic effect by decreasing VEGF production. We also found that the anti-angiogenic effect of CCN1 siRNA came from the reduction in VEGF, which may occur through the reduction in PI3K/Akt, a transcriptional activator of VEGF in ischemic retina.<sup>12</sup> Additionally, our study provides evidence that increased CCN1 contributes to increased levels of PI3K/Akt-VEGF and angiogenesis in OIR retinas, and that CCN1 could be a target for treatment of RNV. Thus, these results suggest that the CCN1-PI3K/Akt-VEGF signaling pathway plays an important role in ROP.

Our study showed that retinal angiogenesis and expression of CCN1, Akt, and VEGF could not be completely inhibited by CCN1 siRNA. This phenomenon may be related to the actions of other angiogenic factors such as bFGF, IGF-1, IL-8, c-Jun, erythropoietin, and HIF-1 $\alpha$ .<sup>31,35,36</sup> Further studies are required to explore the precise relationship of these angiogenic factors with CCN1, and their involvement in these pathological processes.

In conclusion, CCN1 depletion reduced RNV in OIR via PI3K/Akt degradation and subsequent attenuation of VEGF expression. Taken together, our results suggest that CCN1-targeting intervention has therapeutic potential as an anti-angiogenic drug for variable ischemia-induced vasoproliferative retinopathies, especially ROP.

## Acknowledgments

This study was supported by grants from the National Natural Science Foundation of China (No 81371045), the Liaoning Province Technology Foundation of China (No 2010225034), and the Liaoning Province Natural Science Foundation of China (No 20102281).

## Disclosure

All authors declare there are no potential conflicts of interest relevant to this article.

## References

- Nowak-Sliwinska P, Storto M, Cataudella T, et al. Angiogenesis inhibition by the maleimide-based small molecule GNX-686. *Microvasc Res*. 2012;83(2):105–110.
- Semeraro F, Morescalchi F, Duse S, Parmeggiani F, Ganmbicorti E, Costagliola C. Aflibercept in wet AMD: specific role and optimal use. *Drug Des Devel Ther*. 2013;7:711–722.
- Chen J, Stahl A, Hellstrom A, Smith LE. Current update on retinopathy of prematurity: screening and treatment. *Curr Opin Pediatr*. 2011;23(2):173–178.
- Hasan A, Pokeza N, Shaw L, et al. The matricellular protein cysteine-rich protein 61 (CCN1/Cyr61) enhances physiological adaptation of retinal vessels and reduces pathological neovascularization associated with ischemic retinopathy. *J Biol Chem*. 2011;286(11):9542–9554.
- Adamis AP, Shima DT. The role of vascular endothelial growth factor in ocular health and disease. *Retina*. 2005;25(2):111–118.
- Mi XS, Yuan TF, Ding Y, Zhong JX, So XF. Choosing preclinical study models of diabetic retinopathy: key problems for consideration. *Drug Des Devel Ther*. 2014;8:2311–2319.
- Sato T, Kusaka S, Shimojo H, Fujikado T. Vitreous levels of erythropoietin and vascular endothelial growth factor in eyes with retinopathy of prematurity. *Ophthalmology*. 2009;116(9):1599–1603.
- Kuiper EJ, Hughes JM, Van Geest RJ, et al. Effect of VEGF-A on expression of profibrotic growth factor and extracellular matrix genes in the retina. *Invest Ophthalmol Vis Sci*. 2007;48(9):4267–4276.
- Leask A. CCN1: a novel target for pancreatic cancer. *J Cell Commun Signal*. 2011;5(2):123–124.
- Chaour B. New Insights into the Function of the Matricellular CCN1: an Emerging Target in Proliferative Retinopathies. *J Ophthalmic Vis Res*. 2013;8(1):77–82.
- Borkham-Kamphorst E, Schaffrath C, Van de Leur E, et al. The anti-fibrotic effects of CCN1/CYR61 in primary portal myofibroblasts are mediated through induction of reactive oxygen species resulting in cellular senescence, apoptosis and attenuated TGF- $\beta$  signaling. *Biochim Biophys Acta*. 2014;1843(5):902–914.
- You JJ, Yang CH, Yang CM, Chen MS. Cyr61 induces the expression of monocyte chemoattractant protein-1 via the integrin  $\alpha$ 5 $\beta$ 3, FAK, PI3K/Akt, and NF- $\kappa$ B pathways in retinal vascular endothelial cells. *Cell Signal*. 2014;26(1):133–140.
- Koon HW, Shih DQ, Hing TC, et al. Substance P induces CCN1 expression via histone deacetylase activity in human colonic epithelial cells. *Am J Pathol*. 2011;179(5):2315–2326.
- Smith LE, Wesolowski E, McLellan A, et al. Oxygen-induced retinopathy in the mouse. *Invest Ophthalmol Vis Sci*. 1994;35(1):101–111.
- Tolentino M, Mcleod DS, Taomoto M, Otsuji T, Adamis AP, Luttly GA. Pathologic features of vascular endothelial growth factor-induced retinopathy in the nonhuman primate. *Am J Ophthalmol*. 2002;133(3):373–385.
- Chikaraishi Y, Shimazawa M, Hara H. New quantitative analysis, using high-resolution images, of oxygen-induced retinal neovascularization mice. *Exp Eye Res*. 2007;84(3):529–536.

17. Park K, Chen Y, Hu Y, et al. Nanoparticle-mediated expression of an angiogenic inhibitor ameliorates ischemia-induced retinal neovascularization and diabetes-induced retinal vascular leakage. *Diabetes*. 2009;58(8):1902–1913.
18. Livak KJ, Schmittgen TD. Analysis of relative gene expression data using real-time quantitative PCR and the 2(-Delta Delta C(T)) Method. *Methods*. 2001;25(4):402–408.
19. Jiang J, Xia XB, Xu HZ, et al. Inhibition of retinal neovascularization by gene transfer of small interfering RNA targeting HIF-1 $\alpha$  and VEGF. *J Cell Physiol*. 2009;218(1):66–74.
20. Jin Y, An X, Ye Z, Cully B, Wu J, Li J. RGS5, a hypoxia-inducible apoptotic stimulator in endothelial cells. *J Biol Chem*. 2009;284(35):23436–23443.
21. Park SW, Kim JH, Kim KE, et al. Beta-lapachone inhibits pathological retinal neovascularization in oxygen-induced retinopathy via regulation of HIF-1 $\alpha$ . *J Cell Mol Med*. 2014;18(5):875–884.
22. Pakzad-Vaezi K, Albani DA, Kirker AW, et al. A randomized study comparing the efficacy of bevacizumab and ranibizumab as pretreatment for pars plana vitrectomy in proliferative diabetic retinopathy. *Ophthalmic Surg Lasers Imaging Retina*. 2014;45(6):521–524.
23. Hu J, Hoang QV, Chau FY, Blair MP, Lim JJ. Intravitreal anti-vascular endothelial growth factor for choroidal neovascularization in ocular histoplasmosis. *Retin Cases Brief Rep*. 2014;8(1):24–29.
24. Mintz-Hittner HA, Kennedy KA, Chuang AZ; BEAT-ROP Cooperative Group. Efficacy of intravitreal bevacizumab for stage 3+ retinopathy of prematurity. *N Engl J Med*. 2011;364(7):603–615.
25. Vanhaesebrouck S, Daniëls H, Moons L, Vanhole C, Carmeliet P, De Zegher F. Oxygen-induced retinopathy in mice: amplification by neonatal IGF-I deficit and attenuation by IGF-I administration. *Pediatr Res*. 2009;65(3):307–310.
26. Lin M, Chen Y, Jin J, et al. Ischaemia-induced retinal neovascularisation and diabetic retinopathy in mice with conditional knockout of hypoxia-inducible factor-1 in retinal Müller cells. *Diabetologia*. 2011;54(6):1554–1566.
27. Yan L, Chaqour B. Cysteine-rich protein 61 (CCN1) and connective tissue growth factor (CCN2) at the crosshairs of ocular neovascular and fibrovascular disease therapy. *J Cell Commun Signal*. 2013;7(4):253–263.
28. Choi J, Lin A, Shrier E, Lau LF, Grant MB, Chaqour B. Degradome products of the matricellular protein CCN1 as modulators of pathological angiogenesis in the retina. *J Biol Chem*. 2013;288(32):23075–23089.
29. Ren F, Fan M, Mei J, et al. Interferon-gamma and celecoxib inhibit lung-tumor growth through modulating M2/M1 macrophage ratio in the tumor microenvironment. *Drug Des Devel Ther*. 2014;8:1527–1538.
30. Babic AM, Kireeva ML, Kolesnikova TV, Lau LF. CYR61, a product of a growth factor-inducible immediate early gene, promotes angiogenesis and tumor growth. *Proc Natl Acad Sci U S A*. 1998;95(11):6355–6360.
31. You JJ, Yang CH, Chen MS, Yang CM. Cysteine-rich 61, a member of the CCN family, as a factor involved in the pathogenesis of proliferative diabetic retinopathy. *Invest Ophthalmol Vis Sci*. 2009;50(7):3447–3455.
32. Zhang X, Yu W, Dong F. Cysteine-rich 61 (CYR61) is up-regulated in proliferative diabetic retinopathy. *Graefes Arch Clin Exp Ophthalmol*. 2012;250(5):661–668.
33. Hanrahan F, Humphries P, Campbell M. RNAi-mediated barrier modulation: synergies of the brain and eye. *Ther Deliv*. 2010;1(4):587–594.
34. Masuda I, Matsuo T, Yasuda T, Matsuo N. Gene transfer with liposomes to the intraocular tissues by different routes of administration. *Invest Ophthalmol Vis Sci*. 1996;37(9):1914–1920.
35. Narise K, Okuda K, Enomoto Y, Hirayama T, Nagasawa H. Optimization of biguanide derivatives as selective antitumor agents blocking adaptive stress responses in the tumor microenvironment. *Drug Des Devel Ther*. 2014;8:701–717.
36. You JJ, Yang CM, Chen MS, Yang CH. Regulation of Cyr61/CCN1 expression by hypoxia through cooperation of c-Jun/AP-1 and HIF-1 $\alpha$  in retinal vascular endothelial cells. *Exp Eye Res*. 2010;91(6):825–836.

## Supplementary material

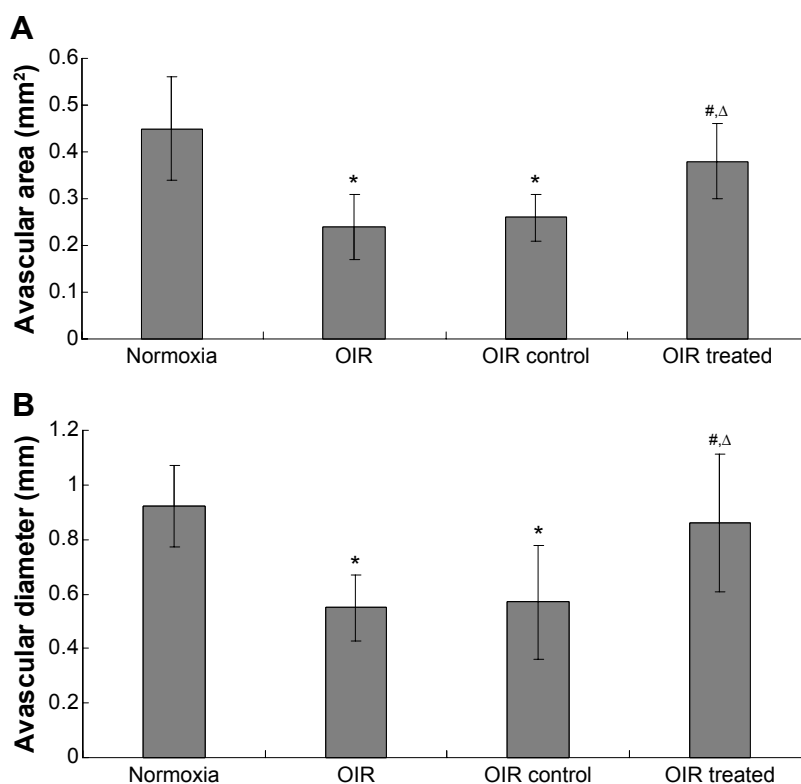


**Figure S1** Examination of avascular area (mm<sup>2</sup>) (A) and avascular diameter (mm) (B) for the every group.

**Notes:** \* $P < 0.05$  versus normoxia group, # $P < 0.05$  versus OIR group,  $\Delta P < 0.05$  versus OIR control group.

**Abbreviation:** OIR, oxygen-induced retinopathy.

Drug Design, Development and Therapy

Dovepress

### Publish your work in this journal

Drug Design, Development and Therapy is an international, peer-reviewed open-access journal that spans the spectrum of drug design and development through to clinical applications. Clinical outcomes, patient safety, and programs for the development and effective, safe, and sustained use of medicines are a feature of the journal, which

has also been accepted for indexing on PubMed Central. The manuscript management system is completely online and includes a very quick and fair peer-review system, which is all easy to use. Visit <http://www.dovepress.com/testimonials.php> to read real quotes from published authors.

Submit your manuscript here: <http://www.dovepress.com/drug-design-development-and-therapy-journal>